

L. I. Solonenko<sup>1</sup>,  
 orcid.org/0000-0003-2092-8044,  
 S. I. Repiakh<sup>2</sup>,  
 orcid.org/0000-0003-0203-4135,  
 K. I. Uzlov<sup>2</sup>,  
 orcid.org/0000-0003-0744-9890,  
 A. V. Dziubina<sup>2</sup>,  
 orcid.org/0000-0002-2215-7231,  
 S. O. Abramov<sup>2</sup>,  
 orcid.org/0000-0003-0675-4850

1 – Odesa Polytechnic State University, Odesa, Ukraine  
 2 – National Metallurgical Academy of Ukraine, Dnipro, Ukraine, e-mail: [123rs@ua.fm](mailto:123rs@ua.fm)

## SAND-SODIUM-SILICATE MIXTURES STRUCTURED IN STEAM-MICROWAVE ENVIRONMENT EFFECTIVE VALUES OF THERMO-PHYSICAL PROPERTIES

**Purpose.** Sand-sodium-silicate mixtures, structured by steam-microwave solidification, thermo-physical properties integral-effective values during Al-Mg alloy and graphite cast iron pouring determination. Sand-sodium-silicate mixture apparent density changing according to quartz sand, clad with sodium silicate solute, fractional composition and its influence on BrA9Zh3L bronze microstructure establishment.

**Methodology.** Quartz sand with 0.23 mm average particle size, sodium silicate solute, aluminum alloy with 8.5 % Mg, flake graphite cast iron SCh200 (DSTU 8833:2019), bronze BrA9Zh3L (GOST 493-79) were used. Mixtures structuring was carried out in 700 W magnetron power microwave furnace. Sand-sodium-silicate mixture thermo-physical properties integral-effective values were calculated by G. A. Anisovich method, using castings results and molds thermography. Structured mixtures apparent density was determined on samples  $\varnothing 50 \times 120$  mm dimension. Metallographic studies were realized using Neophot-21 optical microscope.

**Findings.** It was found that with sodium silicate solute, used for sand cladding, amount increasing from 0.5 to 3 % mold material apparent density decreases and thermal activity lowers. This leads to castings grains size increasing. Mixture sodium silicate solute content was recommended limiting 1.5 % for fine-grained microstructure castings obtaining and clad sand using, which particles pass through mesh side less 0.315 mm sieve. Sands with sodium silicate solute content more than 1.5 %, which don't pass through sieve 0.4 mm mesh side, were recommended as casting molds heat-insulating material using.

**Originality.** For the first time, when aluminum-magnesium alloy and graphite cast iron pouring, quartz sand clad with sodium silicate solute in amount from 0.5 to 3.0 % (weight, over 100 % quartz sand), steam-microwave radiation structured, thermo-physical properties integral-effective values were determined.

**Practical value.** Data obtained using will improve castings solidification time and rate analytical calculations accuracy, forecast level and residual stresses sign in them, shrinkage defects locations. This will reduce casting technology developing time and costs and castings manufacturability.

**Keywords:** *sand-sodium-silicate mixture, steam-microwave solidification, thermo-physical properties, mold, casting, microstructure*

**Introduction.** Cast alloys mechanical and exploitation properties are structurally sensitive. That is, they depend both on alloy chemical composition [1] and on its solidification rate [2, 3]. Alloy solidification rate changing leads to its dendritic structure dispersion changing, its phase components distribution and morphology [4, 5], distance between dendrites secondary axes, quantity of secondary phases [6, 7], etc. All these changes, finally, have a corresponding influence on mechanical, technological and exploitation properties of the cast part.

Solidification rate of almost any casting is largely related to the level of molding and core mixtures thermo-physical properties [8]. These mixtures properties include: specific heat ( $c_2$ ), thermal conductivity ( $\lambda_2$ ), thermal diffusivity ( $a_2$ ), heat storage capacity ( $b_2$ ) and specific density ( $\rho_2$ ). These parameters have been widely used in analytical calculations and computer modeling of casting solidification processes [9, 10], in cast parts quality and material properties prediction [11, 12], etc. At the same time, such forecasts accuracy largely depends on adequacy of casting molds and cores material thermo-physical parameters used values.

At present, data on molds and cores materials thermo-physical parameters are fragmentary, approximate and, as a rule, unregulated. Such data using leads to significant discrepancies between predicted and actual (experimental) re-

sults. That is, such data using as information support for modeling systems is not only unreasonable, but also unacceptable.

**Literature review.** Any material thermo-physical properties feature is their dependence on temperature and, for granular materials, on material apparent density. As a result, under unsteady heat transferring conditions, continuous changing in these parameters consideration is possible only at mixtures thermo-physical properties locally-effective values presence and numerical calculation methods using.

Computation analytical methods give fundamental ideas about complex influence of molds and cores sands thermo-physical parameters on analyzed process, but only for castings of simple configuration (plate, sphere, cylinder, etc.).

For solidification duration and castings in molds cooling analytical calculations, mixtures thermo-physical properties integral-effective values have been used [13, 14]. At the same time, these parameters values are characteristics of mixture only under those solidification conditions and only the casting alloy that has been used in research.

This, in particular, has been evidenced by the data of work [15], given in Tables 1 and 2, for castings with different thicknesses ( $\delta$ ) and with different crystallization temperatures of their material ( $t_{CRT}$ ).

Among above-mentioned thermo-physical parameters for casting in mold solidification duration determination is coefficient  $b_2$ , which A. I. Veinik (1960) calculates by the formula

**Table 1**  
Influence of iron casting thickness ( $\delta$ ) on molding mixture thermo-physical properties

$\delta$ , mm	$\rho_2$ , kg/m <sup>3</sup>	$c_2$ , J/kg·deg	$\lambda_2$ , W/m·deg	$a_2 \cdot 10^6$ , m <sup>2</sup> /s	$b_2$ , W·s <sup>0.5</sup> /m <sup>2</sup> ·deg
10	1700	992	1.100	0.40	1372
20	1760	963	1.380	0.50	1540
30	1720	1030	1.550	0.53	1660
50	1670	1063	1.640	0.56	1708

**Table 2**  
Molding mixture thermo-physical properties for aluminum, cast iron and steel castings

Metal, alloy	$T_{CR}$ , °C	$\rho_2$ , kg/m <sup>3</sup>	$c_2$ , J/kg·deg	$\lambda_2$ , W/m·deg	$b_2$ , W·s <sup>0.5</sup> /m <sup>2</sup> ·deg
Al	660	1400	1070	0.400	775
		1600	1030	0.451	860
		1750	1000	0.518	945
Cast Iron	1147	1400	1300	0.732	1157
		1600	1280	0.715	1210
		1750	1237	0.707	1300
Steel (C = 0.3 %)	1487	1400	1425	0.898	1340
		1600	1425	0.840	1383
		1750	1380	0.828	1420

$$b_2 = 2 \frac{V_{CAST}}{F_{CASM}} \cdot \frac{\rho_1 r}{(t_{CRT} - t_M) \sqrt{\tau_{SOL}}}, \quad (1)$$

where  $V_{CAST}$  – volume of casting;  $F_{CASM}$  – contact area of casting with mold;  $r$  – specific heat of metal (alloy) crystallization;  $t_{CRT}$  – metal (alloy) crystallization temperature;  $\rho_1$  – density of casting solid metal (alloy);  $t_M$  – mold initial temperature;  $\tau_{SOL}$  – casting solidification time.

According to G. A. Anisovich (1960, 1979) data (2)

$$b_2 = 2 \frac{V_{CAST}}{F_{CASM}} \cdot \frac{\rho_1 q_{SOLH}}{(t_{CRT} - t_M) \sqrt{\frac{2n}{n+1} \tau_{SOL}}}; \quad (2)$$

$$q_{SOLH} = q_{OHEAT} + r + \frac{2}{3} c_1 (\vartheta_{SOLET} - \vartheta_{ET});$$

$$\vartheta_{SOLET} = t_{CRT} - t_M, \quad \vartheta_{ET} = t_{OHT} - t_M,$$

where  $q_{SOLH}$  – solidification heat;  $n$  – parabola degree;  $q_{OHEAT}$  – melt overheating heat;  $c_1$  – specific heat of solid metal;  $\vartheta_{SOLET}$  – metal crystallization excess temperature;  $\vartheta_{ET}$  – metal overheating excess temperature;  $t_{OHT}$  – metal overheating temperature.

From formulas (1, 2) analysis it follows that casting solidification time is inversely proportional to  $b_2$  square and (Tables 1 and 2) can vary within fairly wide range due, in particular, to structured mixture apparent density changes. That is, by structured mixture only apparent density value changing, it is possible to significantly change the values of  $\lambda_2$ ,  $b_2$  and, accordingly, casting solidification time and rate.

**Purpose/Problem statement.** Currently, there are no data on integral-effective values of sand-sodium-silicate mixtures (SSSM), structured by of steam-microwave solidification process (SMS-process), thermo-physical properties. Therefore, studies aimed at determining them are relevant.

**Materials and methods.** Quartz sand with an average particle size of 0.23 mm; sodium silicate solute (SSS) with silicate modulus of 2.88–2.93 and specific gravity of 1.42–1.44 g/cm<sup>3</sup>; aluminum alloy with 8.5 % Mg; gray cast iron with flake graphite SCh200 (DSTU 8833:2019); bronze BrA9Zn3L (GOST 493-79) have been used in this study.

For integral-effective values of SSSM thermo-physical properties determination, casting mold has been made according to SMS-process. Structured mixtures were quartz sand cladded with 0.5, 1.5 and 3.0 % SSS (by weight, over 100 % sand).

For structuring, quartz sand has been cladded with sodium silicate solute and poured into polypropylene box. Before sand filling, water charge has been installed at the box bottom – foam urethane sponge saturated with 1–2 g water. At the end of filling sand has been compacted for 10–60 s by vibration with vibration frequency of 50 Hz and amplitude of 0.8–1.0 mm. Cladded sand structuring has been carried out in microwave furnace with magnetron power of 700 W for 12–17 minutes.

Chromel-alumel thermocouples have been used for aluminum-magnesium alloy castings temperature, as well as mold temperature, measuring. Tungsten-molybdenum thermocouple has been used for temperature of gray cast iron casting measuring. Working junction of this thermocouple has been covered with refractory paint layer up to 0.2 mm thick.

All thermocouples have been placed in one horizontal plane of casting mold in accordance with scheme presented in Fig. 1.

Change in thermocouples working junction temperature has been recorded with an electronic potentiometer at recording frequency of 2 s.

Alloys accepted for research have been poured into molds with working cavity dimensions  $\varnothing 30 \times 330$  mm. Obtained data processing and thermo-physical properties integral-effective values calculation of tested mixtures have been carried out according to G. A. Anisovich (1979) method.

Structured mixtures apparent density has been determined on samples  $\varnothing 50 \times 120$  mm and calculated by formula

$$\rho = \frac{m}{V},$$

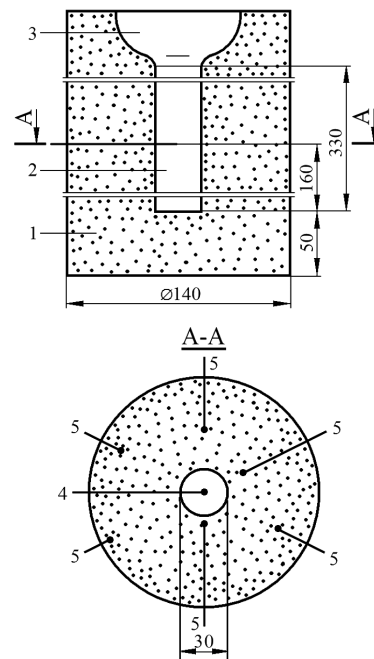


**Fig. 1.** Thermocouples layout in mold:

1 – mold; 2 – casting part; 3 – pouring basin; 4 – central thermocouple; 5 – chromel-alumel thermocouples

where  $m$  – mass of clad mixture;  $V$  – volume occupied by clad mixture.

BrA9Zh3L bronze samples microstructure investigations have been carried out on optical microscope Neophot-21 after their chemical etching in 0.5 % hydrochloric acid aqueous solution. For microstructure investigation, specimens of  $\varnothing 16 \times 130$  mm have been used, which have been poured into steel chill mold, as well as into SSSM structured according to SMS-process.

Specific heat of structured mixtures ( $c_2$ ) has been calculated by formula

$$c_2 = \frac{R\rho_1 r(n+1)}{2X_2\rho_2\vartheta_{ET} \left(1 + \frac{1}{n+2} \cdot \frac{X_2}{R}\right)}, \quad (3)$$

where  $R$  – radius of casting;  $X_2$  – depth of heat penetration into mold body;  $\rho_1$  – alloy specific density in solid state;  $\vartheta_{ET}$  – metal overheating excess temperature.

Structured mixtures thermal conductivity has been calculated by formula

$$\lambda_2 = \frac{R^2(n+2)}{4nt_{CRT}} \left\{ \frac{(n+2)c_2\rho_2}{3(n+1)} \left[ \left(1 + 2 \frac{n+1}{n+2} \cdot \frac{\rho_1 r}{\rho_2 c_2 \vartheta_{ET}}\right)^{\frac{3}{2}} - 1 \right] - \frac{\rho_1 r}{\vartheta_{EA\nu}} \right\}; \quad (4)$$

$$\vartheta_{EA\nu} = \frac{\vartheta_{ET} + \vartheta_{SOLET}}{2}.$$

Calculated value of integral-effective thermal conductivity coefficient has been used for temperature drop in casting determination, and correction has been carried out for values of  $\vartheta_{ET}$  and  $r$  changing.

Coefficient of mold heat storage capacity ( $b_2$ ) has been calculated by formula

$$b_2 = \sqrt{\lambda_2 \cdot c_2 \cdot \rho_2}, \quad (5)$$

and thermal diffusivity ( $a_2$ ) has been calculated by formula,  $m^2/s$

$$a_2 = \frac{\lambda_2}{c_2 \cdot \rho_2}. \quad (6)$$

Thermo-physical parameters values of alloys and their melts overheating during pouring into molds adopted for calculations are given in Table 3.

**Results.** In accordance with accepted research methodology, each cylindrical casting has been thermographed and temperature fields' distributions in molds have been plotted by the time of their solidification completion. As an example, in Fig. 2, *a* shows thermogram of cylindrical casting made of Al + Mg alloy (8.5 %) and temperature distribution in SSSM wall (Fig. 2, *b*), structured by SMS method with 3 % SSS.

From thermogram (Fig. 2, *a*) analysis it follows that heat removal duration of superheat from melt into mold was  $\sim 40$  s,

Table 3

Thermo-physical parameters of alloys and their melts overheating during pouring into molds

Alloy	$t_L, ^\circ\text{C}$	$t_S, ^\circ\text{C}$	$\rho_1, \text{kg/m}^3$	$c_1, \text{J}/(\text{kg} \times \text{deg})$	$c_1', \text{J}/(\text{kg} \times \text{deg})$	$r, \text{kJ/kg}$	$\Delta t_{EP}, ^\circ\text{C}$
Al – Mg (8.5 %)	623	540	2635	950	1160	372	73
SCh 200	1200	1150	7100	560	840	263	80

Note:  $c_1'$  – liquid metal specific heat

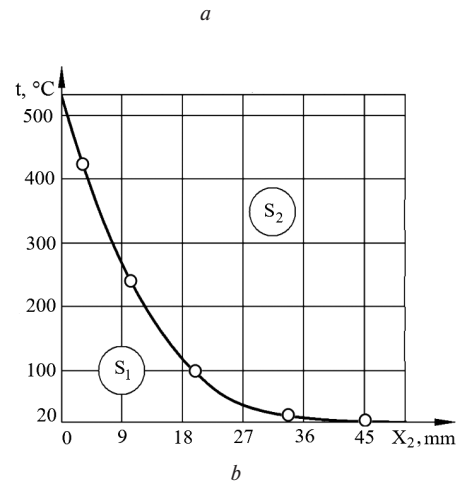
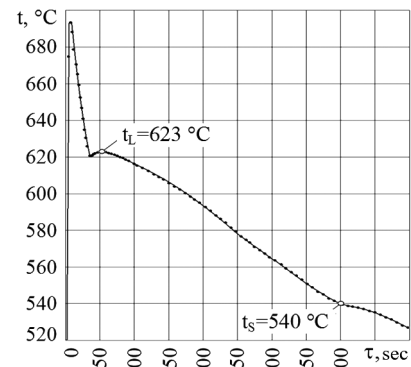


Fig. 2. Thermogram of cylindrical casting made of Al + Mg alloy (8.5 %) solidification (*a*) and temperature distribution in SSSM mold wall with 3 % SSS, structured by SMS method (*b*)

melt undercooling value  $\sim 3$  °C, alloy liquidus temperature  $t_L = 623$  °C, solidus temperature  $t_S = 540$  °C, solidification duration  $\tau_{SOL} = 400$  s, and mold heating depth  $X_2 = 0.047$  m.

Using thermocouples readings and data on their distance from casting surface, temperature distribution curve in form has been built (Fig. 2, *b*). Mold working surface temperature values ( $t_{OHT}$ ) and depth of mold heating ( $X_2$ ) have been determined from results of temperature distribution curve in the mold extrapolation.

Parabola degree ( $n$ ) has been calculated as ratio of image area above ( $S_2$ ) and below ( $S_1$ ) temperature curve. Images areas have been determined from results of their planimetry.

Calculated and experimental parameters values, adopted for computation by formulas (3–6), of thermo-physical properties integral-effective characteristics for structured mixtures, when pouring Al + 8.5 % Mg alloy and gray cast iron SCh 200 into them, are given in Table 4.

Calculating results of structured mixtures thermo-physical properties integral-effective values are given in Tables 5 and 6.

According to Tables 5 and 6 data, dependences  $b_2 = f(m_{SSS})$  (Fig. 3, *a*) and  $\tau_{SOL} = f(m_{SSS})$  (Fig. 3, *b*) for semi-infinite castings  $\varnothing 30$  mm have been plotted.

Thermal conductivity and specific heat dependences on apparent density of casting molds material are shown in Fig. 4.

Molds integral-effective thermal diffusivity and heat storage capacity dependences on apparent density of its material are shown in Fig. 5.

Mold material heat storage capacity integral-effective coefficient dependences on mass of SSS ( $m_{SSS}$ ) used for cladding are shown in Fig. 6, *a*. Semi-infinite cylindrical casting  $\varnothing 30$  mm solidification duration dependences on mold material heat storage capacity coefficient value are shown in Fig. 6, *b*.

Table 4

Calculated and experimental parameters values, adopted for computation when pouring Al + 8.5 % Mg alloy and gray cast iron SCh 200

$m_{SSS}, \%$ (weight)	$\tau_{SOL}, s$	$X_2, m$	$n$	$t_{OHT}, ^\circ C$
Casting from alloy Al + 8.5 % Mg				
0.5	195	0.028	2.9	511
1.5	280	0.036	3.0	507
3.0	400	0.047	3.4	487
Casting from gray cast iron SCh 200				
0.5	137	0.029	3	965
1.5	215	0.04	3.3	960
3.0	317	0.05	3.5	950

Table 5

Thermo-physical properties integral-effective values of structured mixtures, when pouring Al + 8.5 % Mg alloy into them

$m_{SSS}, \%$ (weight)	$\rho_2, \text{kg/m}^3$	$c_2, \frac{J}{\text{kg} \cdot \text{deg}}$	$\lambda_2, \frac{W}{m \cdot \text{deg}}$	$a_2 \cdot 10^6, \frac{m^2}{s}$	$b_2, \frac{W \cdot s^{0.5}}{m^2 \cdot \text{deg}}$
0.5	1758	1047	0.526	0.286	984
1.5	1503	923	0.465	0.335	803
3.0	1380	848	0.414	0.353	696

Table 6

Thermo-physical properties integral-effective values of structured mixtures, when pouring gray cast iron SCh 200 into them

$m_{SSS}, \%$ (weight)	$\rho_2, \text{kg/m}^3$	$c_2, \frac{J}{\text{kg} \cdot \text{deg}}$	$\lambda_2, \frac{W}{m \cdot \text{deg}}$	$a_2 \cdot 10^6, \frac{m^2}{s}$	$b_2, \frac{W \cdot s^{0.5}}{m^2 \cdot \text{deg}}$
0.5	1758	1220	0.801	0.373	1311
1.5	1503	1037	0.689	0.442	1036
3.0	1380	902	0.605	0.486	868

Curves of dependences  $\tau_{SOL} = f(b_2)$ , shows in Fig. 6, *b*. Plots in Fig. 6, *b* analysis shows that both functions agree with formula (2) in terms of casting solidification duration dependence on  $b_2$  value.

Let us represent formula (2) in following form

$$\tau_{SOL} = B \cdot \left( \frac{R}{b_2} \right)^2; \quad (7)$$

$$B = \frac{n+1}{2n} \cdot \left( \frac{\rho_2 \cdot r}{t_{CRT} - t_M} \right)^2.$$

Using formula (7) at  $B = 84 \cdot 10^{10} (W \cdot s)^2 / (m^6 \cdot \text{deg}^2)$  for aluminum alloy and  $B = 10^5 \cdot 10^{10} (W \cdot s)^2 / (m^6 \cdot \text{deg}^2)$  for gray cast iron with relative error no more than 5 %, solidification time of semi-infinite cylindrical casting in SSSM, structured by SMS-process, can be calculated. It has been evidenced by Table 7 data, which shows error ( $\Delta t$ ) values between calculated and experimental values of castings solidification duration.

For data obtained practical using, most acceptable is dependence of structured molding mixture solidification time on specific gravity, shown in Fig. 7, *a*.

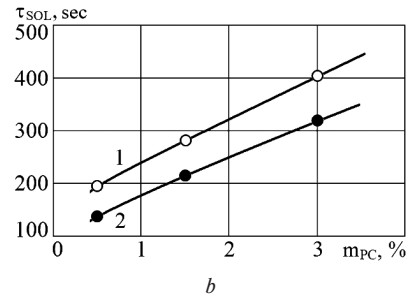
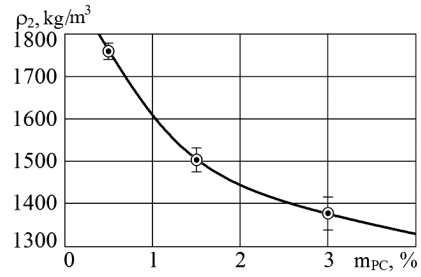


Fig. 3. Dependences of  $\rho_2$  (a) and  $\tau_{SOL}$  (b) on SSS mass used for quartz sand cladding:

1 – castings from alloy Al + 8.5 % Mg; 2 – castings from gray cast iron SCh 200

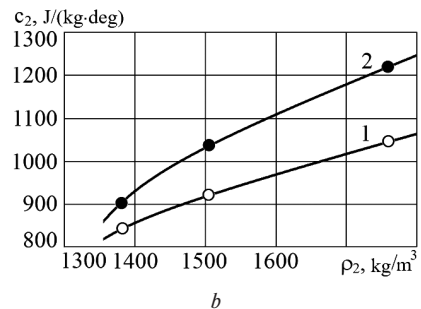
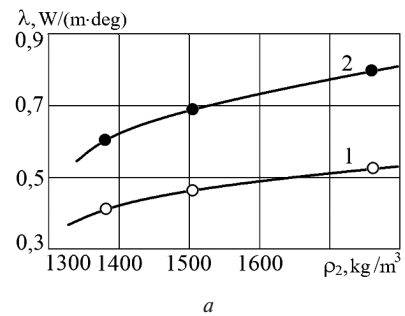
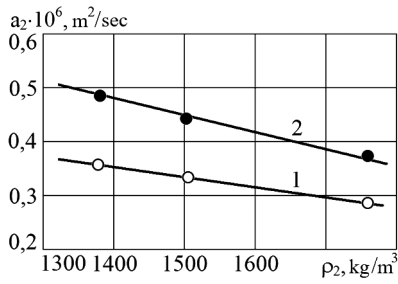


Fig. 4. Dependences of  $\lambda_2$  (a) and  $c_2$  (b) on structured mixture apparent density:

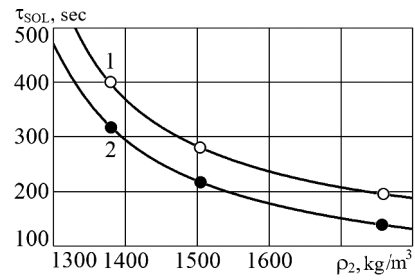
1 – castings from alloy Al + 8.5 % Mg; 2 – castings from gray cast iron SCh 200

It should be taken into account that structured SSSM by SMS method apparent density value also depends on cladded sand particles conglomerates size (dPCS), as evidenced by dependence in Fig. 7, *b*.

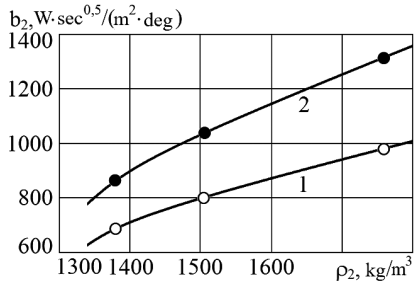
Dependence in Fig. 7, *b* analysis shows that, with pure sand apparent density of 1642 kg/m³, sand-sodium-silicate conglomerates size increasing from 0.1 to 0.8 mm leads to structured mixture apparent density in 2-time decreasing – from ~1610 to ~810 kg/m³. Accordingly, such changes will lead to change in thermo-physical properties of structured mixture. That is, by SSS mass changing in cladded sand or using different sand-sodium-silicate mixture conglomerates fractions, it



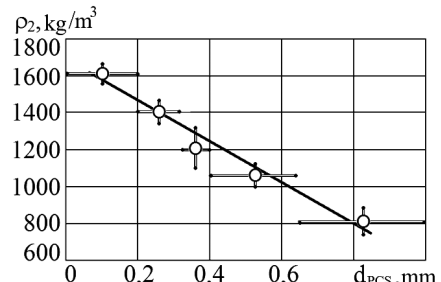
a



a



b



b

Fig. 5. Dependences of  $a_2$  (a) and  $b_2$  (b) on structured mixture apparent density:

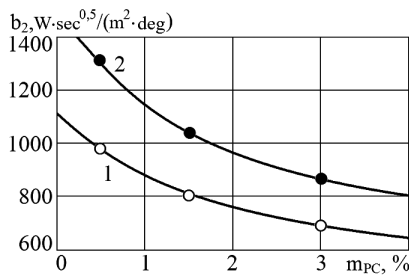
1 – castings from alloy Al + 8.5 % Mg; 2 – castings from gray cast iron SCh 200

Fig. 7. Dependences  $\tau_{SOL}=f(\rho_2)$  (a) and  $\rho_2=f(d_{PCS})$  (b):

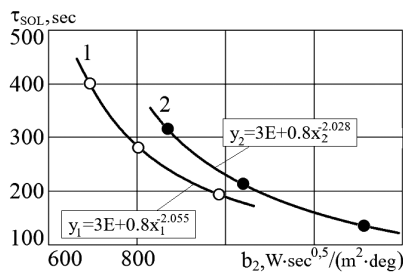
1 – castings from alloy Al + 8.5 % Mg; 2 – castings from gray cast iron SCh 200

is possible to predictably change casting solidification time and, accordingly, alloy structure. This, in particular, is evidenced by microstructures of BrA9Zh3L bronze castings, prepared in various molds, and presented in Fig. 8, and by data in Table 8.

**Conclusions.** For the first time, the thermo-physical properties integral-effective values of quartz sand clad with sodium silicate solute in amount of 0.5 to 3.0 % (by weight, in excess of 100 % quartz sand) and structured by SMS method when pouring aluminum-magnesium alloy and gray cast iron into it have been determined.



a



b

Fig. 6. Dependences  $b_2=f(m_{SS})$  (a) and  $\tau_{SOL}=f(b_2)$  (b):

1 – castings from alloy Al + 8.5 % Mg; 2 – castings from gray cast iron SCh 200

Table 7

Error ( $\Delta t$ ) between calculated and experimental values of castings  $\varnothing 30$  mm from Al + 8.5 % Mg alloy and gray cast iron SCh 200 solidification duration

$b_2$ , W·s <sup>0.5</sup> m <sup>2</sup> ·deg	$\tau_{SOL}$ , (Al + 8.5 % Mg)		$\Delta t$ , %	$b_2$ , W·s <sup>0.5</sup> m <sup>2</sup> ·deg	$\tau_{SOL}$ , (SCh 200)		$\Delta t$ , %
	exper.	calc.			exper.	calc.	
984	195	195.3	-0.2	1311	137	137.5	-0.4
803	280	292.9	-4.6	1036	215	220.1	-2.4
696	400	390.4	2.4	868	317	313.5	1.1

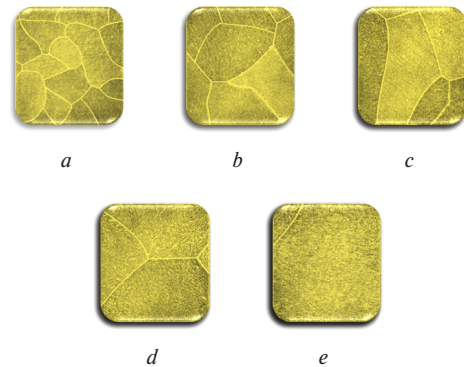


Fig. 8. Specimen  $\varnothing 16 \times 100$  mm of BrA9Zh3L bronze microstructure ( $\times 100$ ) cast into steel chill mold (a) and SSSM, manufactured by SMS-process with SSS content – 0.5 % (b), 1.0 % (c), 1.5 % (d) and 2.5 % (e)

Table 8

Average micrograin size in samples  $\varnothing 18 \times 100$  mm made of BrA9Zh3L bronze cast into various molds

Casting mold	Steel chill mold	SSSM, structured by SMS-process with weight SSS content			
		0.5 %	1 %	1.5 %	2.5 %
D, $\mu\text{m}$	0.12	0.33	0.41	0.50	0.73

Using bronze castings example contained 9 % Al and 3 % Fe, it has been found that sodium silicate solute amount for quartz sand cladding increasing from 0.5 to 3 % leads to castings material micrograin size increasing approximately in ~2.0 times. This regularity is due to intensity of heat removal from solidifying casting into mold decreasing, as evidenced by mixture heat storage capacity value decreasing with amount of silicon silicate solute used for cladding increasing.

To obtain castings with fine-grained structure, SSS content in clad sand should not exceed 1.5 %, and clad sand should pass through sieve with mesh of up to 0.315 mm. Sands with cladding sodium silicate solute content more than 1.5 % and with conglomerate size more than 0.4mm can be used for casting molds heat-insulating elements manufacturing.

When creating refractory heat-insulating materials, it should not be more preferable so much reduce their thermal conductivity integral-effective coefficient, but to decrease their heat storage capacity integral-effective coefficient.

#### References.

1. Mamishev, V.A., Shinsky, O.I., & Sokolovskaya, L.A. (2016). Ways to accelerate the processes of solidification and crystallization in sandy forms. *Materials of the XII International Scientific and Practical Conference "Casting. Metallurgy-2016"*, 159-161. Retrieved from [http://repository.kpi.kharkov.ua/bitstream/KhPI-Press/30304/1/Lite\\_Metallurgiya\\_2016.pdf](http://repository.kpi.kharkov.ua/bitstream/KhPI-Press/30304/1/Lite_Metallurgiya_2016.pdf).
2. Anisovich, A. G., & Andrushevich, A. A. (2018). *Structures of metals and alloys in technological processes of mechanical engineering*. Minsk: Belaruskaya Navuka, 134. ISBN 978-985-08-2363-2.
3. Kotlyarsky, F. M., & Duka, V. M. (2016). Complex influence of hydrogen refining and solidification rate on the structure and mechanical properties of the AK7 alloy. *Casting processes*, 2(116), 9-22. ISSN 2077-1304.
4. Kostryzhev, A. G., Slater, C. D., Marenych, O. O., & Davis, C. L. (2016). Effect of solidification rate on microstructure evolution in dual phase microalloyed steel. *Scientific Reports*, 6, 1-7. <https://doi.org/10.1038/srep35715>.
5. Cai, Z., Zhang, C., Wang, R., Peng, C., Qiu, K., & Wang, N. (2016). Effect of solidification rate on the coarsening behavior of precipitate in rapidly solidified Al – Si alloy. *Progress in Natural Science: Materials International*, 26(4), 391-397. <https://doi.org/10.1016/j.pnsc.2016.08.002>.
6. Brionne, G., Loucif, A., Zhang, C.P., Lapiere-Boire, L. P., & Jahazi, M. (2018). 3D FEM simulation of the effect of cooling rate on SDAS and macrosegregation of a high strength steel. *Materials Science Forum*, 941, 2360-2364. <https://doi.org/10.4028/www.scientific.net/MSF.941.2360>.
7. Ali, M., Porter, D., Kömi, J., Eissa, M., El Faramawy, H., & Matyar, T. (2019). Effect of cooling rate and composition on microstructure and mechanical properties of ultrahigh-strength steels. *Journal of Iron and Steel Research International*, 26, 1350-1365. <https://doi.org/10.1007/s42243-019-00276-0>.
8. Prikhodko, O. G., Deev, V. B., Prusov, E. S., & Kutsenko, A. I. (2020). Influence of the thermophysical characteristics of the alloy and the material of the casting mold on the solidification rate of the castings. *Proceedings of higher educational institutions. Ferrous metallurgy*, 63(5), 327-334. <https://doi.org/10.17073/0368-0797-2020-5-327-334>.
9. Ciesielski, M., & Mochnacki, B. (2019). Comparison of approaches to the numerical modelling of pure metals solidification using the control volume method. *International Journal of Cast Metals Research*, 32(4), 213-220. <https://doi.org/10.1080/13640461.2019.1607650>.
10. Shahane, S., Aluru, N., Ferreira, P., Kapoor, S. G., & Vanka, S. P. (2019). Finite volume simulation framework for die casting with uncertainty quantification. *Applied Mathematical Modelling*, 74, 132-150. <https://doi.org/10.1016/j.apm.2019.04.045>.
11. Hirata, N., & Anzai, K. (2019). Heat transfer and solidification analysis using adaptive resolution particle method. *Materials Transactions*, 60(1), 33-40. <https://doi.org/10.2320/matertrans.MG201807>.
12. Svidró, J., Diószegi, A., & Svidró, J. T. (2020). The origin of thermal expansion differences in various size fractions of silica sand. *International Journal of Cast Metals Research*, 33(6), 242-249. <https://doi.org/10.1080/13640461.2020.1838078>.
13. Krajewski, P. K., Buraś, J., & Piwowarski, G. (2016). Thermal Properties of Foundry Mould Made of Used Green Sand. *Archives of Foundry Engineering*, 16(1), 29-32. <https://doi.org/10.1515/afe-2015-0098>.

14. Lagiewka, M. (2019). Determination of Thermophysical Properties for Selected Molding Sands. *Acta Physica Polonica A*, 136(6), 992-995. <https://doi.org/10.12693/APhysPolA.136.992>.

15. Working properties of mixtures (n.d.). Retrieved from <http://industrial-wood.ru/tehnologiya-liteynogo-proizvodstva/10547-rabochie-svoystva-smesey.html>.

## Теплофізичні властивості піщано-рідкоскляних сумішей після їх структурування в паро-мікрохвильовому середовищі

Л. І. Солоненко<sup>1</sup>, С. І. Пен'ях<sup>2</sup>, К. І. Узлов<sup>2</sup>,  
А. В. Дзюбіна<sup>2</sup>, С. О. Абрамов<sup>2</sup>

1 – Державний університет «Одеська політехніка», м. Одеса, Україна

2 – Національна металургійна академія України, м. Дніпро, Україна, e-mail: [123rs@ua.fm](mailto:123rs@ua.fm)

**Мета.** Визначити інтегрально-ефективні значення теплофізичних властивостей піщано-рідкоскляних сумішей, структурованих способом паро-мікрохвильового затвердіння, при заливці в них сплаву Al-Mg і сірого чавуну. Встановити закономірність зміни уявної щільності піщано-рідкоскляної суміші від фракційного складу кварцового піску, плакованого рідким склом, і його вплив на мікроструктуру бронзи БрА9ЖЗЛ.

**Методика.** У дослідженнях використовували кварцовий пісок із середнім розміром частинок 0,23 мм; натрієве рідке скло; сплав алюмінію з 8,5 % Mg, сірий чавун СЧ 200 (ДСТУ 8833:2019), бронзу БрА9ЖЗЛ (ГОСТ 493-79). Структурування сумішей проводили в мікрохвильовій печі з потужністю магнетрона 700 Вт. Інтегрально-ефективні значення теплофізичних властивостей піщано-рідкоскляної суміші розраховували за методикою Г.А.Анісовича, використовуючи результати термографування виливків і їх ливарних форм. Уявну щільність структурованих сумішей визначали на зразках Ø50 × 120 мм. Металографічні дослідження проводили на оптичному мікроскопі Neophot-21.

**Результати.** Встановлено, що збільшення кількості рідкого скла від 0,5 до 3 % (за масою, понад 100 % піску), що використовують для плакування кварцового піску, знижує уявну щільність матеріалу форми та зменшує її теплову активність, що, відповідно, призводить до збільшення розміру мікрозерен у виливку. Рекомендовано для отримання виливків із дрібнозернистою мікроструктурою вміст рідкого скла в суміші обмежити 1,5 % (за масою, понад 100 % піску) і при цьому використовувати плакований пісок, частинки якого проходять через сито зі стороною осередки до 0,315 мм. Піски із вмістом рідкого скла більше 1,5 % (за масою, понад 100 % піску), що не проходять через сито зі стороною осередки 0,4 мм, рекомендовано використовувати в якості теплоізоляційного матеріалу ливарних форм.

**Наукова новизна.** Вперше при заливці алюмінієво-магнієвого сплаву й сірого чавуну визначені інтегрально-ефективні значення теплофізичних властивостей кварцового піску, плакованого рідким склом у кількості від 0,5 до 3,0 % (за масою, понад 100 % піску) і структурованого в паро-мікрохвильовому середовищі.

**Практична значимість.** Використання отриманих даних дозволить підвищити точність аналітичних розрахунків часу та швидкості затвердіння виливків, прогнозу рівня й знака в них залишкових напружень, місць розташування усадкових дефектів, що скоротить час і витрати на відпрацювання технології лиття та технологічності виливків.

**Ключові слова:** піщано-рідкоскляна суміш, паро-мікрохвильове затвердіння, теплофізичні властивості, виливок, мікроструктура

The manuscript was submitted 29.04.21.